The Q^2 evolution of the Hadronic Photon Structure Function F^γ_2 at LEP

M. Acciarri, P. Achard, O. Adriani, M. Aguilar-Benitez, J. Alcaraz, G. Alemanni, J. Allaby, A. Aloisio, M G. Alviggi, G. Ambrosi, et al.

EUROPEAN ORGANIZATION FOR NUCLEAR RESEARCH

CERN-EP/98-168
21 October 1998

The Q^2 evolution of the Hadronic Photon Structure Function F_2^γ at LEP

The L3 Collaboration

Abstract

New measurements at a centre-of-mass energy $\sqrt{s} \simeq 183$ GeV of the hadronic photon structure function $F_2^\gamma(x)$ in the Q^2 interval, 9 GeV$^2 \leq Q^2 \leq 30$ GeV^2, are presented. The data, collected in 1997 with the L3 detector, correspond to an integrated luminosity of 51.9 pb^{-1}. Combining with the data taken at a centre-of-mass energy of 91 GeV, the evolution of F_2^γ with Q^2 is measured in the Q^2 range from 1.2 GeV^2 to 30 GeV^2. F_2^γ shows a linear growth with $\ln Q^2$; the value of the slope $\alpha^{-1} \mathrm{d}F_2^\gamma(Q^2)/\mathrm{d}\ln Q^2$ is measured in two x bins from 0.01 to 0.2 and is somewhat higher than predicted.

Submitted to *Phys. Lett. B*

1 Introduction

The hadronic photon structure function is measured at e^+e^- storage rings via the interaction of two virtual photons $e^+e^- \to e^+e^-\gamma^*\gamma \to e^+e^-$hadrons [1–3] where one of the scattered electrons[1)] is detected (single tag). Here we present a new measurement obtained at LEP with the L3 detector at $\sqrt{s} \simeq 183$ GeV for an integrated luminosity of 51.9 pb^{-1}. This measurement is an extension of the study at $\sqrt{s} \simeq 91$ GeV with an integrated luminosity of 140 pb^{-1} detailed in Ref. [3].

The structure functions of the photon are extracted in a deep inelastic scattering (DIS) process $e\gamma \to eX$ from the differential cross-section $d^2\sigma/dxdQ^2$. The photon (γ^*) of high virtuality, Q^2, is used as a probe for the structure of the quasi-real target photon (γ) with virtuality $P^2 \sim 0$. In the kinematic regime studied here ($E_{tag} \sim E_{beam}$) the measured cross-section is only sensitive to one structure function, $F_2^\gamma(x, Q^2)$. The Bjorken variable $x = Q^2/(Q^2 + P^2 + W_{\gamma\gamma}^2)$ requires the measurement of the two-photon centre-of-mass energy $W_{\gamma\gamma}$ which is obtained from the measurement of the effective mass of the hadronic system.

In the quark parton model (QPM) the contribution to F_2^γ comes from the diagram $\gamma^*\gamma \to q\bar{q}$. Contrary to the structure functions of hadrons containing valence quarks, as for example the proton structure function, F_2^p, the QPM produces a large value of F_2^γ at large x and an increase with Q^2 at any value of x. In reality the photon can fluctuate into partonic states and in particular into vector mesons (Vector Dominance Model, VDM). Thus the overall contribution to F_2^γ is more complicated and different sets of parton distributions in the photon are available. Also QCD corrections (gluon radiation) modify both the QPM and VDM parts of F_2^γ. As for F_2^p, the biggest uncertainty comes from the gluon distribution which dominates the low x region. At LEP we have access to low values of x, $0.002 < x < 0.2$ at $\sqrt{s} \simeq 91$ GeV and $0.01 < x < 0.5$ with the present data at $\sqrt{s} \simeq 183$ GeV.

2 Monte Carlo models

Three different Monte Carlo generators are used in this study: PHOJET [4], TWOGAM [5] and the generator of Vermaseren (JAMVG) [6].

PHOJET is an event generator for pp, γp and $\gamma\gamma$ interactions, described within the Dual Parton Model (DPM). In PHOJET the charm quark is treated as massless, but it is only generated for $W_{\gamma\gamma} > 7$ GeV.

In JAMVG, the QED processes $e^+e^- \to e^+e^-f\bar{f}$ are generated via the two-photon interaction. Since the charm quark is not well simulated in PHOJET and is more important in the high Q^2 region, we use PHOJET for the light quark contributions and JAMVG for the charm quark contribution[2)], contrary to the previous analysis [3] where only PHOJET was used.

TWOGAM generates three different processes separately: the QPM, the VDM and the QCD resolved photon contribution. A transverse momentum cut-off, $p_t^{cut} = 3.5$ GeV, is applied to separate soft and hard processes [7]. The transverse momentum cut-off has been increased relative to that of the previous data ($p_t^{cut} = 2.3$ GeV [3]) since the latter cut produces a too large cross-section for hard processes in the high Q^2 region [8].

The dominant background sources to the reaction $e^+e^- \to e^+e^-$hadrons are $e^+e^- \to e^+e^-\tau^+\tau^-$, simulated by JAMVG [6], and $e^+e^- \to$ hadrons, simulated by PYTHIA [9]. The

[1)] Electron stands for electron or positron throughout this paper.

[2)] In the following text as well as in the figures the label PHOJET means always PHOJET+JAMVG ($c\bar{c}$)

other backgrounds are $e^+e^- \to \tau^+\tau^-$, simulated by KORALZ [10], and $e^+e^- \to W^+W^-$, simulated by KORALW [11].

All Monte Carlo events are passed through a full detector simulation using the GEANT [12] and the GEISHA [13] programs and are reconstructed in the same way as the data.

3 Data Analysis

3.1 Event Selection

A detailed description of the L3 detector is given in Ref. [14]. The single tagged two-photon hadronic events are triggered by two independent triggers: the central track trigger [15] (77% of events with an efficiency of 76%) and the single tag trigger [16] (94% of events with an efficiency of 92%). The central track trigger requires at least two charged particles, each with $p_t > 150$ MeV, back-to-back in the transverse plane within 60°. The single tag trigger requires at least 70 GeV deposited in one of the small angle electromagnetic calorimeters, in coincidence with at least one track in the central tracking chamber. The total trigger efficiency is $98 \pm 1\%$ which takes into account also the high level software triggers [17] and is almost independent of the visible mass of the hadronic final state.

Single tagged two-photon hadronic event candidates are selected by similar cuts to the one applied in the previous analysis [3] with some modifications due to the higher beam energy:

- A tagged electron is identified as the highest energy cluster in one of the small angle electromagnetic calorimeters with $E_{tag} > 70$ GeV and a polar angle in the range 30 mrad $< \theta_{tag} <$ 66 mrad. The anti-tag condition is kept the same as for the previous measurement [3], $E_{anti-tag} < 12$ GeV for the most energetic cluster opposite to the tagged electron.

- The number of charged particles must be greater than two.

- The visible invariant mass, W_{vis}, of the hadronic final state is required to be greater than 3 GeV. The transverse momentum component of the hadronic state perpendicular to the tag plane, p_t^{out}, and the momentum balance, p_t^{bal}, have to be less than 5 GeV. The tag plane is defined by the beam axis and the tagged electron direction. Definitions of W_{vis}, p_t^{out} and p_t^{bal} are given in Ref. [3].

- The total energy deposited in the calorimeters must be less than 50 GeV.

After the selection cuts, a total of 1694 events is selected in the Q^2 range 9 GeV$^2 \leq Q^2 \leq$ 30 GeV^2. The sample is divided into three Q^2 bins of similar statistics: 9 GeV$^2 \leq Q^2 <$ 13 GeV^2, 13 GeV$^2 \leq Q^2 <$ 18 GeV^2 and 18 GeV$^2 \leq Q^2 \leq$ 30 GeV^2. Table 1 shows the numbers of selected events and expected background events, dominated by $e^+e^- \to e^+e^-\tau^+\tau^-$. The contaminations from $e^+e^- \to$ hadrons, $e^+e^- \to \tau^+\tau^-$ and $e^+e^- \to W^+W^-$ are negligible.

To improve the measurement of W_{vis}, we include the kinematics of the tagged electron in the visible mass calculation and define W_{rec} by using the constraint of transverse momentum conservation as suggested in Ref. [18].

The distributions for the variables W_{rec}, Q^2, x_{vis} and x_{rec} are shown in Fig. 1. The variables x_{vis} and x_{rec} are calculated from W_{vis} and W_{rec}. Both PHOJET and TWOGAM give a reasonable description of the data. The energy flow versus the pseudorapidity, $\eta = -\ln(\tan(\theta/2))$ where θ is the polar angle of final state particles, is shown for three Q^2 intervals in Fig. 2. The

tag direction is always on the negative side and the energy of the tagged electron is not shown in the plot. The agreement between data and the different Monte Carlo predictions is good except at pseudorapidity values, $\eta > 3$ and $\eta < -1$.

3.2 Extraction of F_2^γ

To calculate the double differential cross-section $\mathrm{d}^2\sigma/\mathrm{d}x\mathrm{d}Q^2$ the data are subdivided into three x bins in the interval 9 GeV$^2 \leq Q^2 <$ 13 GeV^2 and into four x bins in the other two Q^2 intervals. They are corrected with the same unfolding technique [19] as used in Ref. [3, 20]. The structure function F_2^γ is then extracted as described in detail in Ref. [21]. The values of F_2^γ/α obtained by unfolding the data with PHOJET are given in Table 2, where α is the fine-structure constant. The unfolding procedure gives strong correlations between neighbouring bins. For example the correlations between the lowest x bin and the adjacent, and next-to-adjacent bins are 60% and 40%, respectively. Since the Q^2 is well measured ($\Delta Q^2/Q^2 = 2\%$), the correlations between Q^2 bins are negligible.

The systematic errors are given in Table 2, these include:

- The uncertainties due to the selection procedure which are estimated by varying the selection cuts. The uncertainties from the individual selection cuts are added in quadrature.
- The effect of the discrepancies at pseudorapidity values, $\eta > 3$ and $\eta < -1$, are estimated by removing these regions from the extraction of F_2^γ. The difference is found to be negligible.
- The difference of F_2^γ obtained using x_{rec} or x_{vis} is used as an estimate of the unfolding uncertainty. The differences are in general smaller than 10%.
- The results obtained by correcting the data with TWOGAM are consistent. The differences are given in Table 2 as a separate systematic error.

The values of F_2^γ/α are not corrected for the fact that P^2 is not strictly equal to zero since the non-zero P^2 effect depends on the unknown mixture of point-like and hadronic photon coupling in the data [3]. As a consequence the values given in Table 2 are smaller than the values extrapolated to $P^2 = 0$, as can be seen in Ref. [21, 22].

The values of $F_2^\gamma\alpha$ in the three different Q^2 intervals are compared to the predictions of SaS-1d [22], GRV-LO (low order) [23], GRV-HO (high order) [23] and LAC1 [24] in Fig. 3. At low x the predictions of GRV and SaS-1d lie below the measured F_2^γ values and LAC1 is too large. It was already pointed out in Ref. [25] that the existing parametrisations do not fulfil the QCD sum rule for leading twist partonic distributions of real and virtual photon targets, since the data available to determine these parametrisations were not sensitive to the gluon distributions in the photon. Following this consideration the authors of LAC1 constructed F_2^γ by rescaling the proton structure function, using the Gribov factorisation [26]. The new predictions [27] obtained in our x and Q^2 ranges are similar to the SaS-1d prediction. The agreement between the data and the different parametrisations is good at high x, where they all give similar values.

3.3 The Q^2 evolution of F_2^γ

The Q^2 evolution of F_2^γ is studied by using our previous measurements at $\sqrt{s} \simeq 91$ GeV [3] and the present measurements at $\sqrt{s} \simeq 183$ GeV. The Q^2 values range from 1.2 GeV^2 to 30 GeV^2.

The measured values of F_2^γ/α are shown in Fig. 4 as a function of Q^2. The expected linear growth with $\ln Q^2$ is observed. The new measurement at high Q^2 ($9\ \mathrm{GeV}^2 \leq Q^2 \leq 30\ \mathrm{GeV}^2$) agrees well with our previous measurement at low Q^2 ($1.2\ \mathrm{GeV}^2 \leq Q^2 \leq 9\ \mathrm{GeV}^2$) [3]. The function $a+b\ln Q^2$ is fitted to the data in the first two x bins ($0.01 < x < 0.1$ and $0.1 < x < 0.2$) taking into account the statistical and systematic errors from the data selection and unfolding. The fit results are:

$$F_2^\gamma(Q^2)/\alpha = (0.13 \pm 0.01 \pm 0.02) + (0.080 \pm 0.009 \pm 0.009) \times \ln(Q^2/\mathrm{GeV}^2)$$
$$\text{for } 0.01 < x < 0.1\ , \qquad (\chi^2/dof = 3.43/5)$$

and

$$F_2^\gamma(Q^2)/\alpha = (0.04 \pm 0.08 \pm 0.08) + (0.13 \pm 0.03 \pm 0.03) \times \ln(Q^2/\mathrm{GeV}^2)$$
$$\text{for } 0.1 < x < 0.2\ , \qquad (\chi^2/dof = 0.25/2)$$

The correlation coefficients of the fit are -0.9 in $0.01 < x < 0.1$ and -0.97 in $0.1 < x < 0.2$. The second error on the coefficients gives the uncertainties from the Monte Carlo models, estimated by repeating the fit with values unfolded with TWOGAM. These values are compatible with the result, $b = 0.10 \pm 0.02^{+0.05}_{-0.02}$, obtained by OPAL [2] in the Q^2 range from 7.5 GeV^2 to 135 GeV^2 and the adjacent x interval $0.1 < x < 0.6$.

The predictions of GRV, SaS-1d and LAC1 are also shown in Fig. 4. The slopes of different parametrisations, obtained by the same fit, are summarised in Table 3. For the lowest x interval ($0.01 < x < 0.1$) the slope predicted by LAC1 is much larger than our fitted value as we discussed before. The one predicted by SaS-1d is too low. The results of the fit indicate also that the slope increases with x in the interval $0.01 < x < 0.2$ because of the contribution of the QPM process. In the case of the proton structure function, F_2^p, the slope decreases with increasing x.

4 Conclusions

The photon structure function F_2^γ has been measured at LEP with the L3 detector at $\sqrt{s} \simeq 183$ GeV. The measurement is done in the Q^2 interval from 9 GeV^2 to 30 GeV^2. The x range is $0.01 < x < 0.5$. The data show a reasonable agreement with the TWOGAM and PHOJET Monte Carlo models.

Our data are compared to the parametrisations of the photon structure function F_2^γ which were determined from the low energy data. At low values of x, the data are above the predictions of the GRV and SaS-1d models and below the prediction of the LAC1 model, indicating that the gluon density in the photon structure function is underestimated in the GRV and SaS-1d and overestimated in the LAC1 model.

Combining the present results at $\sqrt{s} \simeq 183$ GeV with the data taken at $\sqrt{s} \simeq 91$ GeV, the Q^2 evolution is studied in the Q^2 range from 1.2 GeV^2 to 30 GeV^2 in the low x region ($x < 0.2$) where the gluon contribution to the structure function is dominant. The measurements at the two different centre-of-mass energies are consistent. The $\ln Q^2$ evolution is clearly observed in the data. At low x, the rise of F_2^γ is larger than predicted by the GRV and SaS-1d models, thus requiring a modification of the gluon density in the photon structure function F_2^γ.

Acknowledgements

We express our gratitude to the CERN accelerator divisions for the excellent performance of the LEP machine. We acknowledge with appreciation the effort of all engineers, technicians and support staff who have participated in the construction and maintenance of this experiment.

References

[1] PLUTO Coll., C. Berger *et al.*, Phys. Lett. **B 142** (1984) 111;
TASSO Coll., M. Althoff *et al.*, Z. Phys. **C 31** (1986) 527;
TPC/2γ Coll., H. Aihara *et al.*, Z. Phys. **C 34** (1987) 1;
TOPAZ Coll., K. Muramatsu *et al.*, Phys. Lett. **B 332** (1994) 477;
AMY Coll., S.K. Sahu *et al.*, Phys. Lett. **B 346** (1995) 208;
DELPHI Coll., P. Abreu *et al.*, Z. Phys. **C 69** (1996) 223.

[2] OPAL Coll., R. Akers *et al.*, Z. Phys. **C 61** (1994) 199;
OPAL Coll., K. Ackerstaff *et al.*, Z. Phys. **C 74** (1997) 33;
OPAL Coll., K. Ackerstaff *et al.*, Phys. Lett. **B 411** (1997) 387;
OPAL Coll., K. Ackerstaff *et al.*, Phys. Lett. **B 412** (1997) 225.

[3] L3 Coll., M. Acciarri *et al.*, Preprint CERN-EP/98-098, Phys. Lett. B accepted.

[4] PHOJET version 1.05c is used.
R. Engel, Z. Phys. **C 66** (1995) 203;
R. Engel and J. Ranft, Phys. Rev. **D 54** (1996) 4244.

[5] TWOGAM version 1.71 is used.
S. Nova *et al.*, DELPHI Note 90-35 (1990).
We thank our colleagues from DELPHI to make their program available to us.

[6] J.A.M. Vermaseren, Nucl. Phys. **B 229** (1983) 347.

[7] J.H. Field, F. Kapusta and L. Poggioli, Phys. Lett. **B 181** (1986) 362;
J.H. Field, F. Kapusta and L. Poggioli, Z. Phys. **C 36** (1987) 121.

[8] C.H. Lin, L3 Note 2298 (1998). This L3 Note is freely available on request from: The L3 secretariat, CERN, CH-1211 Geneva 23, Switzerland. Internet: http://l3www.cern.ch.

[9] T. Sjöstrand, Comp. Phys. Comm. **82** (1994) 74.

[10] S. Jadach, B.F.L. Ward and Z. Wąs, Comp. Phys. Comm. **79** (1994) 503.

[11] M. Skrzypek, S. Jadach, W. Placzek and Z. Wąs, Comp. Phys. Comm. **94** (1996) 216;
M. Skrzypek, S. Jadach, M. Martinez, W. Placzek and Z. Wąs, Phys. Lett. **B 372** (1996) 289.

[12] R. Brun *et al.*, GEANT 3.15 preprint CERN DD/EE/84-1 (Revised 1987).

[13] H. Fesefeldt, RWTH Aachen report PITHA 85/2 (1985). This program allows for the effects of energy loss, multiple scattering, decays and interactions in the detector material, as well as for time-dependent detector effects.

[14] L3 Collab., B. Adeva *et al.*, Nucl. Inst. Meth. **A 289** (1990) 35;
M. Acciarri *et al.*, Nucl. Inst. Meth. **A 351** (1994) 300;
M. Chemarin *et al.*, Nucl. Inst. Meth. **A 349** (1994) 345;
I.C. Brock *et al.*, Nucl. Inst. Meth. **A 381** (1996) 236;
A. Adam *et al.*, Nucl. Inst. Meth. **A 383** (1996) 342.

[15] P. Béné *et al.*, Nucl. Inst. Meth. **A 306** (1991) 150.

[16] R. Bizzarri *et al.*, Nucl. Inst. Meth. **A 283** (1989) 799.

[17] C. Dionisi *et al.*, Nucl. Inst. Meth. **A 336** (1993) 78;
Y. Bertsch *et al.*, Nucl. Inst. Meth. **A 340** (1994) 309;
Y. Bertsch *et al.*, Nucl. Inst. Meth. **A 340** (1994) 322.

[18] L. Lönnblad *et al.*, "$\gamma\gamma$ event generators", in Physics at LEP2, ed. G. Altarelli, T. Sjöstrand and F. Zwirner, CERN 96-01 (1996), Volume 2, 201.

[19] G. D'Agostini, Nucl. Inst. Meth. **A 362** (1996) 489.

[20] L3 Coll., M. Acciarri *et al.*, Phys. Lett. **B 408** (1997) 450.

[21] L3 Coll., M. Acciarri *et al.*, Preprint CERN-EP/98-060, Phys. Lett. B accepted.

[22] G.A. Schuler and T. Sjöstrand, Z. Phys. **C 68** (1995) 607;
G.A. Schuler and T. Sjöstrand, Phys. Lett. **B 376** (1996) 193.

[23] M. Glück, E. Reya and A. Vogt, Phys. Rev. **D 45** (1992) 3986;
M. Glück, E. Reya and A. Vogt, Phys. Rev. **D 46** (1992) 1973.

[24] H. Abramowicz, K. Charchula and A. Levy, Phys. Lett. **B 269** (1991) 458.

[25] L.L. Frankfurt and E.G. Gurvich, Phys. Lett. **B 386** (1996) 379.

[26] V.N. Gribov and L.Ya. Pomeranchuk, Phys. Rev. Lett. **8** (1962) 343.

[27] H. Abramowicz, E. Gurvich and A. Levy, Phys. Lett. **B 420** (1998) 104.

The L3 Collaboration:

M.Acciarri,[27] P.Achard,[19] O.Adriani,[16] M.Aguilar-Benitez,[26] J.Alcaraz,[26] G.Alemanni,[22] J.Allaby,[17] A.Aloisio,[29] M.G.Alviggi,[29] G.Ambrosi,[19] H.Anderhub,[48] V.P.Andreev,[7,37] T.Angelescu,[13] F.Anselmo,[10] A.Arefiev,[28] T.Azemoon,[3] T.Aziz,[11] P.Bagnaia,[36] L.Baksay,[43] A.Balandras,[4] R.C.Ball,[3] S.Banerjee,[11] Sw.Banerjee,[11] K.Banicz,[45] A.Barczyk,[48,46] R.Barillère,[17] L.Barone,[36] P.Bartalini,[22] M.Basile,[10] R.Battiston,[33] A.Bay,[22] F.Becattini,[16] U.Becker,[15] F.Behner,[48] J.Berdugo,[26] P.Berges,[15] B.Bertucci,[33] B.L.Betev,[48] S.Bhattacharya,[11] M.Biasini,[33] A.Biland,[48] G.M.Bilei,[33] J.J.Blaising,[4] S.C.Blyth,[34] G.J.Bobbink,[2] R.Bock,[1] A.Böhm,[1] L.Boldizsar,[14] B.Borgia,[17,36] D.Bourilkov,[48] M.Bourquin,[19] S.Braccini,[19] J.G.Branson,[39] V.Brigljevic,[48] F.Brochu,[4] I.C.Brock,[34] A.Buffini,[16] A.Buijs,[44] J.D.Burger,[15] W.J.Burger,[33] J.Busenitz,[43] A.Button,[3] X.D.Cai,[15] M.Campanelli,[48] M.Capell,[15] G.Cara Romeo,[10] G.Carlino,[29] A.M.Cartacci,[16] J.Casaus,[26] G.Castellini,[16] F.Cavallari,[36] N.Cavallo,[29] C.Cecchi,[19] M.Cerrada,[26] F.Cesaroni,[23] M.Chamizo,[26] Y.H.Chang,[50] U.K.Chaturvedi,[18] M.Chemarin,[25] A.Chen,[50] G.Chen,[8] G.M.Chen,[8] H.F.Chen,[20] H.S.Chen,[8] X.Chereau,[4] G.Chiefari,[29] L.Cifarelli,[38] F.Cindolo,[10] C.Civinini,[16] I.Clare,[15] R.Clare,[15] G.Coignet,[4] A.P.Colijn,[2] N.Colino,[26] S.Costantini,[9] F.Cotorobai,[13] B.de la Cruz,[26] A.Csilling,[14] T.S.Dai,[15] J.A.van Dalen,[31] R.D'Alessandro,[16] R.de Asmundis,[29] P.Deglon,[19] A.Degré,[4] K.Deiters,[46] D.della Volpe,[29] P.Denes,[35] F.DeNotaristefani,[36] A.De Salvo,[48] M.Diemoz,[36] D.van Dierendonck,[2] F.Di Lodovico,[48] C.Dionisi,[17,36] M.Dittmar,[48] A.Dominguez,[39] A.Doria,[29] M.T.Dova,[18,♯] D.Duchesneau,[4] D.Dufournand,[4] P.Duinker,[2] I.Duran,[40] S.Easo,[33] H.El Mamouni,[25] A.Engler,[34] F.J.Eppling,[15] F.C.Erné,[2] P.Extermann,[19] M.Fabre,[46] R.Faccini,[36] M.A.Falagan,[26] S.Falciano,[36] A.Favara,[16] J.Fay,[25] O.Fedin,[37] M.Felcini,[48] T.Ferguson,[34] F.Ferroni,[36] H.Fesefeldt,[1] E.Fiandrini,[33] J.H.Field,[19] F.Filthaut,[17] P.H.Fisher,[15] I.Fisk,[39] G.Forconi,[15] L.Fredj,[19] K.Freudenreich,[48] C.Furetta,[27] Yu.Galaktionov,[28,15] S.N.Ganguli,[11] P.Garcia-Abia,[6] M.Gataullin,[32] S.S.Gau,[12] S.Gentile,[36] N.Gheordanescu,[13] S.Giagu,[36] S.Goldfarb,[22] Z.F.Gong,[20] G.Gratta,[32] M.W.Gruenewald,[9] R.van Gulik,[2] V.K.Gupta,[35] A.Gurtu,[11] L.J.Gutay,[45] D.Haas,[6] B.Hartmann,[1] A.Hasan,[30] D.Hatzifotiadou,[10] T.Hebbeker,[9] A.Hervé,[17] P.Hidas,[14] J.Hirschfelder,[34] H.Hofer,[48] G. Holzner,[48] H.Hoorani,[34] S.R.Hou,[50] I.Iashvili,[47] B.N.Jin,[8] L.W.Jones,[3] P.de Jong,[17] I.Josa-Mutuberría,[26] R.A.Khan,[18] D.Kamrad,[47] J.S.Kapustinsky,[24] M.Kaur,[18,◇] M.N.Kienzle-Focacci,[19] D.Kim,[36] D.H.Kim,[42] J.K.Kim,[42] S.C.Kim,[42] W.W.Kinnison,[24] A.Kirkby,[32] D.Kirkby,[32] J.Kirkby,[17] D.Kiss,[14] W.Kittel,[31] A.Klimentov,[15,28] A.C.König,[31] A.Kopp,[47] I.Korolko,[28] V.Koutsenko,[15,28] R.W.Kraemer,[34] W.Krenz,[1] A.Kunin,[15,28] P.Lacentre,[47,♮,♯] P.Ladron de Guevara,[26] I.Laktineh,[25] G.Landi,[16] C.Lapoint,[15] K.Lassila-Perini,[48] P.Laurikainen,[21] A.Lavorato,[38] M.Lebeau,[17] A.Lebedev,[15] P.Lebrun,[25] P.Lecomte,[48] P.Lecoq,[17] P.Le Coultre,[48] H.J.Lee,[9] J.M.Le Goff,[17] R.Leiste,[47] E.Leonardi,[36] P.Levtchenko,[37] C.Li,[20] C.H.Lin,[50] W.T.Lin,[50] F.L.Linde,[2,17] L.Lista,[29] Z.A.Liu,[8] W.Lohmann,[47] E.Longo,[36] W.Lu,[32] Y.S.Lu,[8] K.Lübelsmeyer,[1] C.Luci,[17,36] D.Luckey,[15] L.Luminari,[36] W.Lustermann,[48] W.G.Ma,[20] M.Maity,[11] G.Majumder,[11] L.Malgeri,[17] A.Malinin,[28] C.Maña,[26] D.Mangeol,[31] P.Marchesini,[48] G.Marian,[43,¶] J.P.Martin,[25] F.Marzano,[36] G.G.G.Massaro,[2] K.Mazumdar,[11] R.R.McNeil,[7] S.Mele,[17] L.Merola,[29] M.Meschini,[16] W.J.Metzger,[31] M.von der Mey,[1] D.Migani,[10] A.Mihul,[13] H.Milcent,[17] G.Mirabelli,[36] J.Mnich,[17] P.Molnar,[9] B.Monteleoni,[16] T.Moulik,[11] R.Mount,[32] G.S.Muanza,[25] F.Muheim,[19] A.J.M.Muijs,[2] S.Nahn,[15] M.Napolitano,[29] F.Nessi-Tedaldi,[48] H.Newman,[32] T.Niessen,[1] A.Nippe,[22] A.Nisati,[36] H.Nowak,[47] Y.D.Oh,[42] G.Organtini,[36] R.Ostonen,[21] C.Palomares,[26] D.Pandoulas,[1] S.Paoletti,[36,17] P.Paolucci,[29] H.K.Park,[34] I.H.Park,[42] G.Pascale,[36] G.Passaleva,[17] S.Patricelli,[29] T.Paul,[12] M.Pauluzzi,[33] C.Paus,[17] F.Pauss,[48] D.Peach,[17] M.Pedace,[36] Y.J.Pei,[1] S.Pensotti,[27] D.Perret-Gallix,[4] B.Petersen,[31] S.Petrak,[9] A.Pevsner,[5] D.Piccolo,[29] M.Pieri,[16] P.A.Piroué,[35] E.Pistolesi,[27] V.Plyaskin,[28] M.Pohl,[48] V.Pojidaev,[28,16] H.Postema,[15] J.Pothier,[17] N.Produit,[19] D.Prokofiev,[37] J.Quartieri,[38] G.Rahal-Callot,[48] N.Raja,[11] P.G.Rancoita,[27] M.Rattaggi,[27] G.Raven,[39] P.Razis,[30] D.Ren,[48] M.Rescigno,[36] S.Reucroft,[12] T.van Rhee,[44] S.Riemann,[47] K.Riles,[3] A.Robohm,[48] J.Rodin,[43] B.P.Roe,[3] L.Romero,[26] S.Rosier-Lees,[4] S.Roth,[1] J.A.Rubio,[17] D.Ruschmeier,[9] H.Rykaczewski,[48] S.Sakar,[36] J.Salicio,[17] E.Sanchez,[26] M.P.Sanders,[31] M.E.Sarakinos,[21] C.Schäfer,[1] V.Schegelsky,[37] S.Schmidt-Kaerst,[1] D.Schmitz,[1] N.Scholz,[48] H.Schopper,[49] D.J.Schotanus,[31] J.Schwenke,[1] G.Schwering,[1] C.Sciacca,[29] D.Sciarrino,[19] L.Servoli,[33] S.Shevchenko,[32] N.Shivarov,[41] V.Shoutko,[28] J.Shukla,[24] E.Shumilov,[28] A.Shvorob,[32] T.Siedenburg,[1] D.Son,[42] B.Smith,[15] P.Spillantini,[16] M.Steuer,[15] D.P.Stickland,[35] A.Stone,[7] H.Stone,[35] B.Stoyanov,[41] A.Straessner,[1] K.Sudhakar,[11] G.Sultanov,[18] L.Z.Sun,[20] H.Suter,[48] J.D.Swain,[18] Z.Szillasi,[43,¶] X.W.Tang,[8] L.Tauscher,[6] L.Taylor,[12] C.Timmermans,[31] Samuel C.C.Ting,[15] S.M.Ting,[15] S.C.Tonwar,[11] J.Tóth,[14] C.Tully,[35] K.L.Tung,[8] Y.Uchida,[15] J.Ulbricht,[48] E.Valente,[36] G.Vesztergombi,[14] I.Vetlitsky,[28] G.Viertel,[48] S.Villa,[12] M.Vivargent,[4] S.Vlachos,[6] H.Vogel,[34] H.Vogt,[47] I.Vorobiev,[17,28] A.A.Vorobyov,[37] A.Vorvolakos,[30] M.Wadhwa,[6] W.Wallraff,[1] J.C.Wang,[15] X.L.Wang,[20] Z.M.Wang,[20] A.Weber,[1] S.X.Wu,[15] S.Wynhoff,[1] Z.Z.Xu,[20] B.Z.Yang,[20] C.G.Yang,[8] H.J.Yang,[8] M.Yang,[8] J.B.Ye,[20] S.C.Yeh,[51] J.M.You,[34] An.Zalite,[37] Yu.Zalite,[37] P.Zemp,[48] Y.Zeng,[1] Z.P.Zhang,[20] G.Y.Zhu,[8] R.Y.Zhu,[32] A.Zichichi,[10,17,18] F.Ziegler,[47] G.Zilizi.[43,¶]

1 I. Physikalisches Institut, RWTH, D-52056 Aachen, FRG§
III. Physikalisches Institut, RWTH, D-52056 Aachen, FRG§
2 National Institute for High Energy Physics, NIKHEF, and University of Amsterdam, NL-1009 DB Amsterdam, The Netherlands
3 University of Michigan, Ann Arbor, MI 48109, USA
4 Laboratoire d'Annecy-le-Vieux de Physique des Particules, LAPP,IN2P3-CNRS, BP 110, F-74941 Annecy-le-Vieux CEDEX, France
5 Johns Hopkins University, Baltimore, MD 21218, USA
6 Institute of Physics, University of Basel, CH-4056 Basel, Switzerland
7 Louisiana State University, Baton Rouge, LA 70803, USA
8 Institute of High Energy Physics, IHEP, 100039 Beijing, China△
9 Humboldt University, D-10099 Berlin, FRG§
10 University of Bologna and INFN-Sezione di Bologna, I-40126 Bologna, Italy
11 Tata Institute of Fundamental Research, Bombay 400 005, India
12 Northeastern University, Boston, MA 02115, USA
13 Institute of Atomic Physics and University of Bucharest, R-76900 Bucharest, Romania
14 Central Research Institute for Physics of the Hungarian Academy of Sciences, H-1525 Budapest 114, Hungary‡
15 Massachusetts Institute of Technology, Cambridge, MA 02139, USA
16 INFN Sezione di Firenze and University of Florence, I-50125 Florence, Italy
17 European Laboratory for Particle Physics, CERN, CH-1211 Geneva 23, Switzerland
18 World Laboratory, FBLJA Project, CH-1211 Geneva 23, Switzerland
19 University of Geneva, CH-1211 Geneva 4, Switzerland
20 Chinese University of Science and Technology, USTC, Hefei, Anhui 230 029, China△
21 SEFT, Research Institute for High Energy Physics, P.O. Box 9, SF-00014 Helsinki, Finland
22 University of Lausanne, CH-1015 Lausanne, Switzerland
23 INFN-Sezione di Lecce and Universitá Degli Studi di Lecce, I-73100 Lecce, Italy
24 Los Alamos National Laboratory, Los Alamos, NM 87544, USA
25 Institut de Physique Nucléaire de Lyon, IN2P3-CNRS,Université Claude Bernard, F-69622 Villeurbanne, France
26 Centro de Investigaciones Energéticas, Medioambientales y Tecnologícas, CIEMAT, E-28040 Madrid, Spain♭
27 INFN-Sezione di Milano, I-20133 Milan, Italy
28 Institute of Theoretical and Experimental Physics, ITEP, Moscow, Russia
29 INFN-Sezione di Napoli and University of Naples, I-80125 Naples, Italy
30 Department of Natural Sciences, University of Cyprus, Nicosia, Cyprus
31 University of Nijmegen and NIKHEF, NL-6525 ED Nijmegen, The Netherlands
32 California Institute of Technology, Pasadena, CA 91125, USA
33 INFN-Sezione di Perugia and Universitá Degli Studi di Perugia, I-06100 Perugia, Italy
34 Carnegie Mellon University, Pittsburgh, PA 15213, USA
35 Princeton University, Princeton, NJ 08544, USA
36 INFN-Sezione di Roma and University of Rome, "La Sapienza", I-00185 Rome, Italy
37 Nuclear Physics Institute, St. Petersburg, Russia
38 University and INFN, Salerno, I-84100 Salerno, Italy
39 University of California, San Diego, CA 92093, USA
40 Dept. de Fisica de Particulas Elementales, Univ. de Santiago, E-15706 Santiago de Compostela, Spain
41 Bulgarian Academy of Sciences, Central Lab. of Mechatronics and Instrumentation, BU-1113 Sofia, Bulgaria
42 Center for High Energy Physics, Adv. Inst. of Sciences and Technology, 305-701 Taejon, Republic of Korea
43 University of Alabama, Tuscaloosa, AL 35486, USA
44 Utrecht University and NIKHEF, NL-3584 CB Utrecht, The Netherlands
45 Purdue University, West Lafayette, IN 47907, USA
46 Paul Scherrer Institut, PSI, CH-5232 Villigen, Switzerland
47 DESY-Institut für Hochenergiephysik, D-15738 Zeuthen, FRG
48 Eidgenössische Technische Hochschule, ETH Zürich, CH-8093 Zürich, Switzerland
49 University of Hamburg, D-22761 Hamburg, FRG
50 National Central University, Chung-Li, Taiwan, China
51 Department of Physics, National Tsing Hua University, Taiwan, China
§ Supported by the German Bundesministerium für Bildung, Wissenschaft, Forschung und Technologie
‡ Supported by the Hungarian OTKA fund under contract numbers T019181, F023259 and T024011.
¶ Also supported by the Hungarian OTKA fund under contract numbers T22238 and T026178.
♭ Supported also by the Comisión Interministerial de Ciencia y Tecnología.
♯ Also supported by CONICET and Universidad Nacional de La Plata, CC 67, 1900 La Plata, Argentina.
♮ Supported by Deutscher Akademischer Austauschdienst.
♢ Also supported by Panjab University, Chandigarh-160014, India.
△ Supported by the National Natural Science Foundation of China.

Q^2 [GeV^2]	selected	background
9 – 13	656	24
13 – 18	498	21
18 – 30	540	26

Table 1: The number of selected events in three Q^2 intervals at $\sqrt{s} \simeq 183$ GeV. The dominant background is $e^+e^- \to e^+e^-\tau^+\tau^-$.

$\langle Q^2 \rangle$ [GeV^2]	x range	F_2^γ/α	Model
10.8	0.01 – 0.1	$0.30 \pm 0.02 \pm 0.03$	+0.0
	0.1 – 0.2	$0.35 \pm 0.03 \pm 0.02$	+0.0
	0.2 – 0.3	$0.30 \pm 0.04 \pm 0.10$	+0.03
15.3	0.01 – 0.1	$0.37 \pm 0.02 \pm 0.03$	+0.0
	0.1 – 0.2	$0.42 \pm 0.04 \pm 0.01$	−0.02
	0.2 – 0.3	$0.42 \pm 0.05 \pm 0.05$	+0.05
	0.3 – 0.5	$0.35 \pm 0.05 \pm 0.08$	+0.13
23.1	0.01 – 0.1	$0.40 \pm 0.03 \pm 0.03$	−0.02
	0.1 – 0.2	$0.44 \pm 0.04 \pm 0.04$	+0.0
	0.2 – 0.3	$0.47 \pm 0.05 \pm 0.02$	+0.01
	0.3 – 0.5	$0.44 \pm 0.05 \pm 0.11$	+0.05

Table 2: The measured values of F_2^γ/α as a function of x in three Q^2 intervals. $\langle Q^2 \rangle$ is the average of Q^2 in the intervals 9 GeV$^2 \leq Q^2 <$ 13 GeV^2, 13 GeV$^2 \leq Q^2 <$ 18 GeV^2 and 18 GeV$^2 \leq Q^2 \leq$ 30 GeV^2. The data are unfolded with PHOJET. The first error is statistical. The second error is the systematic error from the data selection and unfolding. The last column is the difference between the results obtained with PHOJET and TWOGAM.

x range	0.01 - 0.1	0.1 - 0.2
data (L3)	$0.080 \pm 0.009 \pm 0.009$	$0.13 \pm 0.03 \pm 0.03$
GRV-LO	0.065	0.064
GRV-HO	0.061	0.063
SaS-1d	0.043	0.055
LAC1	0.255	0.065

Table 3: Comparison of the $\ln Q^2$ dependence, parameter b of the fit, obtained by fitting the data and the different theoretical parametrisations of F_2^γ/α.

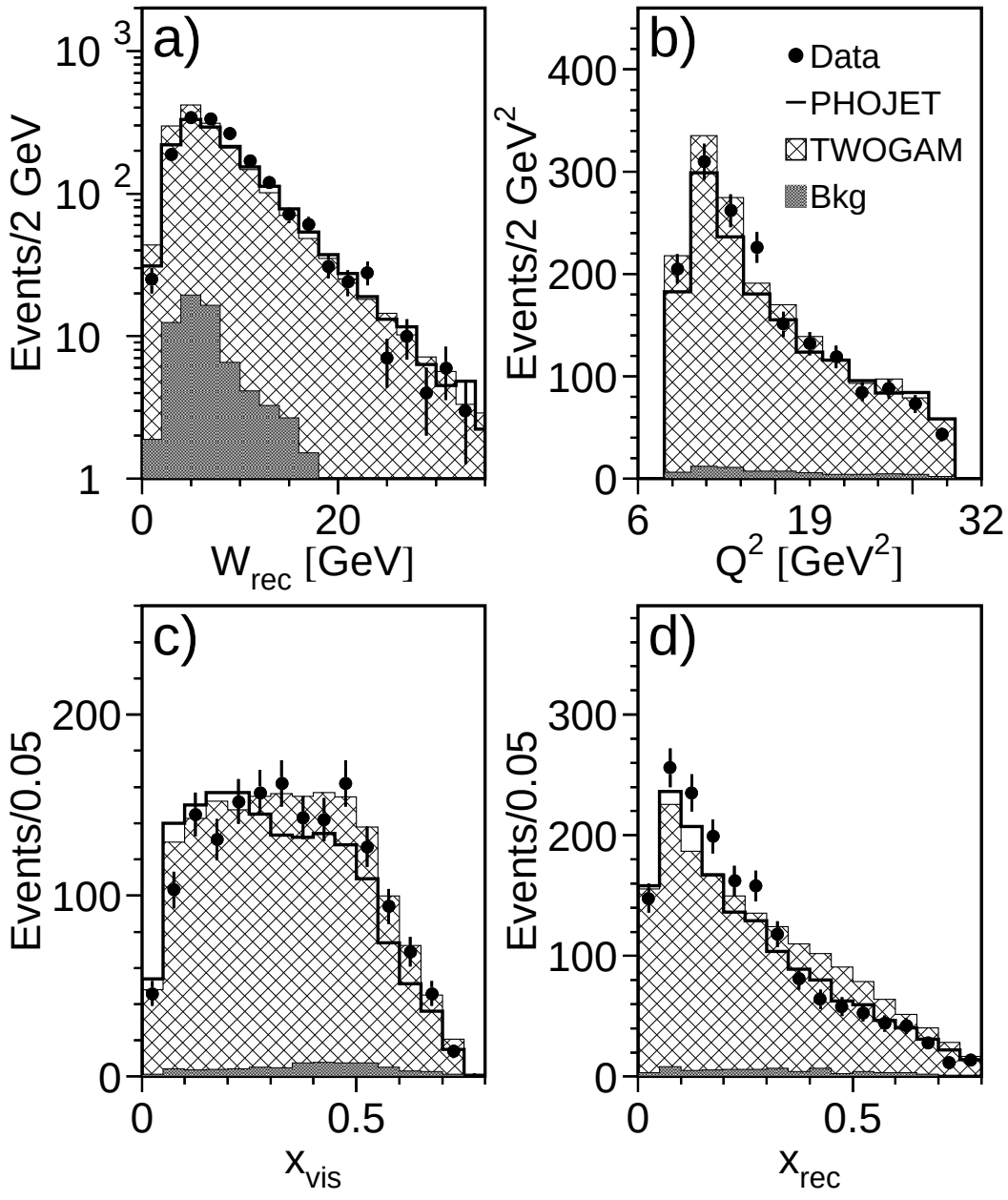

Figure 1: Distributions of a) W_{rec}, b) Q^2 of the tagged electron, c) x_{vis} and d) x_{rec}. The data are compared to the Monte Carlo predictions, normalised to the data luminosity. The dominant background is $e^+e^- \to e^+e^-\tau^+\tau^-$.

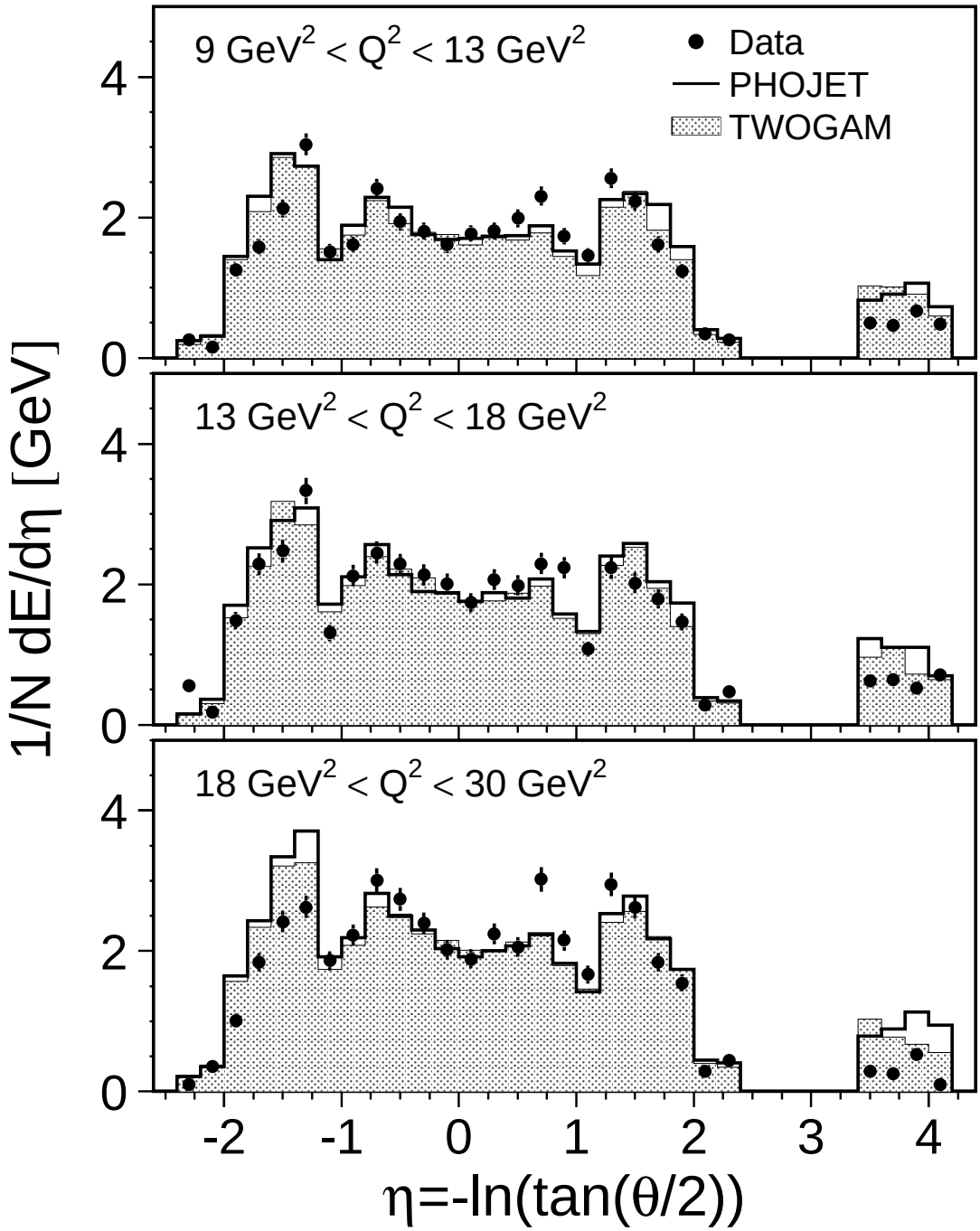

Figure 2: Hadronic energy flow as a function of the pseudorapidity η in the different Q^2 intervals after background subtraction. The tagged electron direction is always on the negative side.

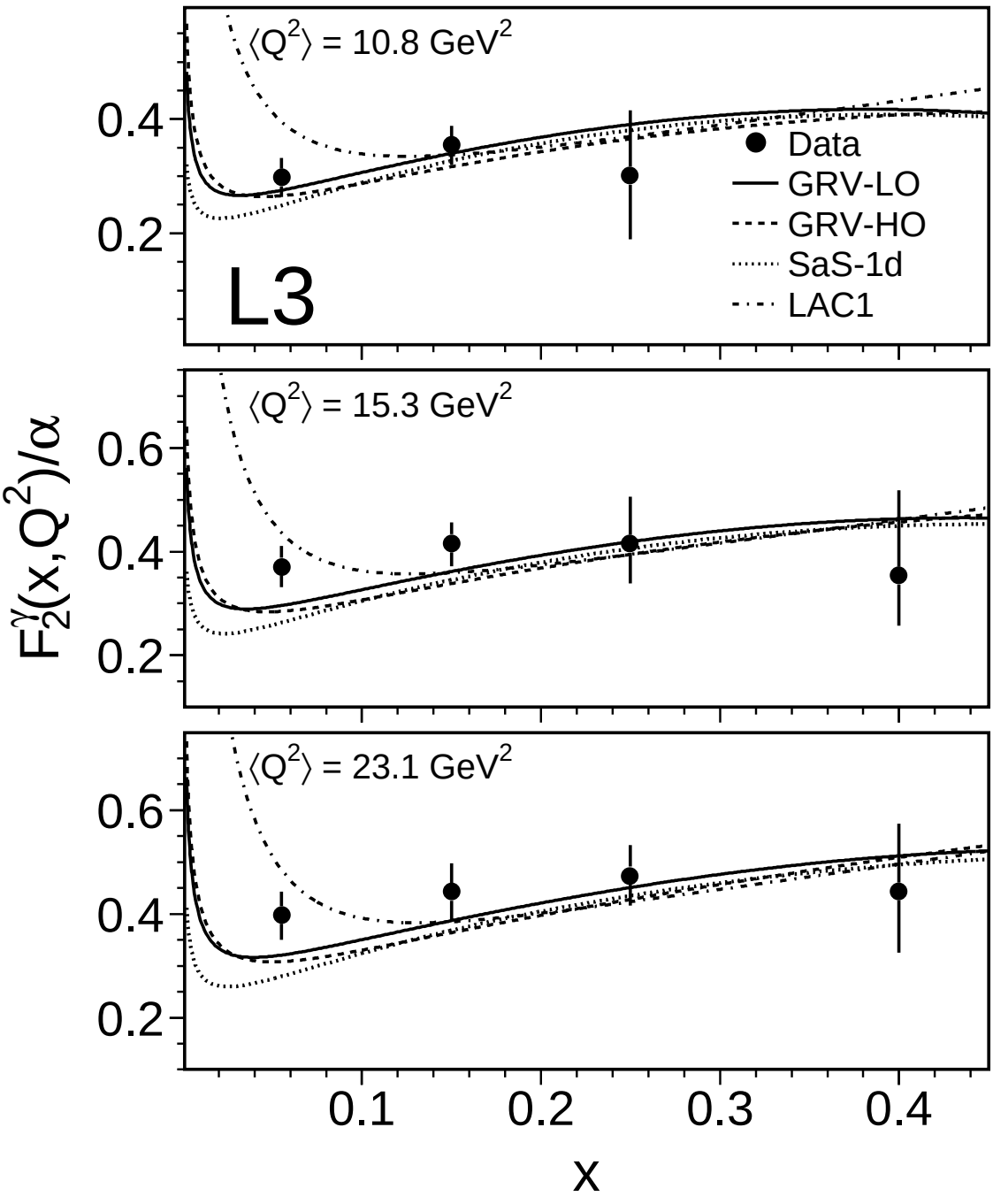

Figure 3: Measured values of F_2^γ/α at $\langle Q^2\rangle = 10.8$ GeV^2, $\langle Q^2\rangle = 15.3$ GeV^2 and $\langle Q^2\rangle = 23.1$ GeV^2 as a function of x. The data are unfolded with PHOJET. The statistical and systematic errors are added in quadrature. The data are compared to the predictions of GRV [23], SaS-1d [22] and LAC1 [24].

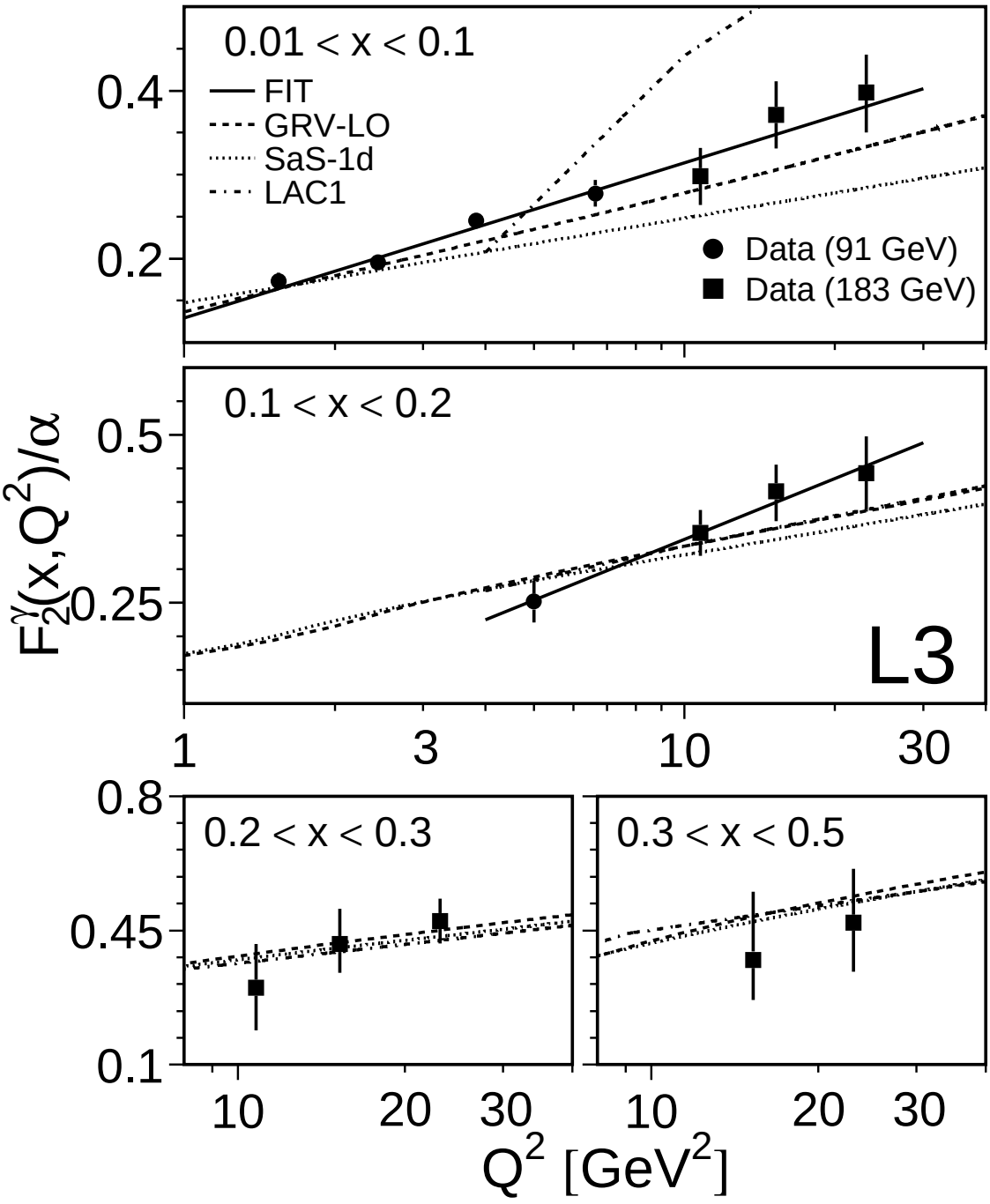

Figure 4: Measured values of F_2^γ/α as a function of Q^2 compared to the predictions of GRV-LO [23], SaS-1d [22] and LAC [24] in four x bins. GRV-HO is similar to GRV-LO. The data are unfolded with PHOJET. The solid line is a fit to the data with the function $a + b \ln Q^2$. The statistical and systematic errors are added in quadrature.